mathematics

MDPI

Article

A Simulation Optimization Framework for Dynamic Vessel Diversion Under Port Closure Disruptions

Yeon Ho Cha [1], Yunjee Kim [2], Minsu Woo [3], Jeongeum Kim [3], Sewoong Oh [2,*] and Sung Won Cho [1,3,*]

[1] Department of Management Engineering, Dankook University, Cheonan 31116, Republic of Korea; cyh1348@dankook.ac.kr
[2] Maritime Digital Transformation Research Center, Korea Research Institute of Ships and Ocean Engineering (KRISO), Daejeon 34103, Republic of Korea; yunjee0531@kriso.re.kr
[3] Department of Industrial Engineering, Dankook University, Cheonan 31116, Republic of Korea; woosu@dankook.ac.kr (M.W.); jeumkim@dankook.ac.kr (J.K.)
* Correspondence: osw@kriso.re.kr (S.O.); sungwon.cho@dankook.ac.kr (S.W.C.)

Abstract

This study develops a simulation optimization framework for dynamic vessel diversion under port closure disruptions. The framework considers centralized diversion decisions based on the queue threshold at the primary port, diversion probability, and reception capacity at the alternative port. A discrete-event simulation model is developed using 2024 vessel call data from Busan and Gwangyang Ports. Total logistics cost comprises vessel time, fuel, transportation, and cargo time costs. A total of 211 diversion policies are evaluated across eight closure durations ranging from 12 to 96 h, using 300 selection replications with common random numbers. The selected policies are then assessed using 300 independent evaluation replications. Sensitivity analysis considers low, medium, and high cargo time values derived from published commodity benchmarks. The results show that the preferred diversion policy depends on closure duration and cargo time value, and that diversion is not always economically beneficial during short closures. For a 96 h closure, the selected policies reduce mean total logistics cost relative to no diversion by 3.21%, 12.80%, and 21.26% under low, medium, and high cargo time values, respectively. These policies also reduce the mean maximum queue length at the primary port by 18.47% to 30.31% and shorten the time from reopening until the last retained vessel arriving during the closure starts service by 12.12 to 19.63 h. However, waiting times increase for vessels originally bound for the alternative port. The findings support coordinated diversion policies that balance congestion relief and logistics costs across both ports.

Keywords: vessel diversion; disruption management; port congestion; simulation optimization; discrete-event simulation

MSC: 90B06; 90B22; 90-10

Check for updates

Academic Editor: Gaige Wang

Received: 12 October 2026
Revised: 8 November 2026
Accepted: 13 November 2026
Published: 17 November 2026

Copyright: © 2026 by the authors. Licensee MDPI, Basel, Switzerland. This article is an open access article distributed under the terms and conditions of the Creative Commons Attribution (CC BY) license.

1. Introduction

More than 80% of global merchandise trade by volume is carried by sea [1], and ports serve as critical nodes connecting global supply chains [2]. Port performance depends not only on facility capacity but also on information sharing, intermodal transportation, and logistics functions [3–5]. Therefore, disruptions at major ports can affect freight flows across domestic and international logistics networks [2].

Globally, 86% of ports are exposed to more than three types of natural hazards, with associated annual port-specific risk estimated at approximately USD 7.5 billion. Tropical cyclones account for approximately 32% of this risk [6]. Strong winds during typhoons can restrict vessel berthing and port operations, resulting in substantial economic losses [7]. Diverting vessels and cargo to alternative ports can be considered to maintain freight flows during temporary port closures [8].

However, vessel diversion incurs additional logistics costs. Diverted vessels require additional sailing time and fuel to reach alternative ports. Additional transportation costs arise when transshipment cargo must be returned to the primary port for onward shipping or when export cargo must be transferred from the primary port to an alternative port. Furthermore, the handling capacity and hinterland transportation conditions of alternative ports constrain the feasible scale of diversion [8]. Previous research has also found that substitution between ports can be limited during short disruptions [9].

When vessels remain at the primary port during a closure, vessel queues and unprocessed cargo accumulate. After operations resume, the accumulated vessels and newly arriving vessels compete for limited berth capacity, potentially prolonging port congestion [10,11]. Vessel diversion can reduce waiting times and cargo delays at the primary port, but may also increase congestion at the alternative port. Therefore, the economic benefit of diversion depends on whether the reduction in vessel and cargo time costs outweighs the additional sailing, transportation, and waiting costs associated with diversion [12,13].

Previous studies have examined alternative port selection, cargo rerouting, and predefined vessel diversion allocations under disruptions [8,12,14]. These approaches mainly focus on alternative destination selection or predetermined cargo and vessel allocations rather than diversion decisions based on the observed queue conditions at each vessel arrival. Therefore, it is necessary to evaluate dynamic diversion policies that consider changing port congestion and alternative port capacity during disruptions.

In this study, we develop a simulation optimization framework for dynamic vessel diversion under port closure disruptions. The framework considers a state-based diversion policy under centralized decision-making. The policy determines the diversion eligibility of each arriving vessel based on the queue threshold at the primary port and available reception capacity at the alternative port. Eligible vessels are diverted according to a specified diversion probability. Capacity reservations for vessels en route to the alternative port are also considered. A discrete-event simulation (DES) model is developed to represent stochastic vessel arrivals, service times, and queueing processes at both ports. Candidate diversion policies are evaluated under different closure durations and cargo time values using total logistics cost, including vessel time, fuel, transportation, and cargo time costs. The policy with the lowest estimated mean cost among the evaluated candidates is selected for each condition. The effects of diversion on congestion and vessel waiting times at both ports are also analyzed. This study examines when vessel diversion reduces total logistics cost and how the selected queue threshold and diversion probability vary with closure duration and cargo time value. The analysis considers congestion relief at the primary port, additional sailing and interport inland transportation costs, and increased waiting at the alternative port.

The remainder of this paper is organized as follows. Section 2 reviews the relevant literature on port disruptions, congestion, vessel diversion, and port resilience, and presents the contributions of this study. Section 3 describes the problem, diversion policy, and simulation optimization model. Section 4 presents the case study, experimental design, and simulation results. Finally, Section 5 summarizes the conclusions and directions for future research.

2. Literature Review

2.1. Port Disruptions and Congestion

Previous studies have examined the economic effects of port closures, including regional losses, costs incurred by port stakeholders, and risks associated with natural hazards [6,7,15]. Rose and Wei [15] analyzed the economic consequences of port closures and the effects of resilience measures. Zhang et al. [7] estimated the losses incurred by ports, shipping companies, and shippers during typhoon disruptions. Verschuur et al. [6] assessed exposure to multiple natural hazards and the resulting infrastructure, trade, and logistics risks at 1340 ports worldwide.

The duration and effects of port disruptions have also been investigated using operational data. Verschuur et al. [9] examined 141 disruption instances involving 74 ports and 27 natural disasters using automatic identification system (AIS) data. For cases involving port closure, the median duration of the overall disruption impact was six days, and the 95th percentile was 22.2 days. These durations include recovery after closure and should not be interpreted as periods of complete port closure. The study also found limited substitution between ports during short disruptions. Therefore, alternative port capacity and operating conditions should be considered when evaluating diversion.

Port congestion has been studied using queueing theory and simulation [11,16–18]. A port can be represented as a queueing system in which vessels arrive stochastically and are served by a limited number of berths. Under comparable operating conditions, vessel waiting times increase with utilization and can rise sharply as demand approaches service capacity [10]. Related research has examined port size and allocation [19], container terminal operations [16], container stacking strategies [20,21], berth and quay crane scheduling [22], ship and berth system performance [11], port congestion [18], and the management of berth crane resources [17].

2.2. Port Diversion and Resilience

Previous studies have examined port diversion primarily from the perspective of cargo redistribution and alternative transport arrangements under disruptions. Port choice models have identified alternative destinations by considering transportation costs, cargo time values, and handling capacities [8], while network-based optimization models have determined cargo assignments under disruptions to port and transport link capacities [12]. These approaches support the allocation of cargo across available transport networks but do not explicitly address vessel diversion decisions based on evolving port congestion.

Operational simulation has also been used to evaluate port responses under crisis conditions. Martagan et al. [14] modeled vessel arrivals, port services, and inland container transportation to assess alternative vessel allocations in terms of cargo lead times and congestion. However, diversion proportions were predetermined rather than adjusted according to the queue conditions observed at individual vessel arrivals.

Related research on port resilience has examined how operational capacity, vessel responses, and recovery strategies affect port performance during disruptions. Existing studies have addressed governance and collaboration in resilience management [23], port cluster responses to typhoons through vessel skipping and changes in cargo handling capacity [24], and network resilience under recurrent hazards [25]. More broadly, restoration optimization under recurrent dependent hazards has been investigated [26]. Although these studies provide insights into disruption management and operational resilience, they do not explicitly integrate arrival-level vessel diversion decisions with the evolving queueing processes and logistics costs of both the primary and alternative ports.

2.3. Research Contributions

Table 1 distinguishes three research perspectives. The first group examines capacity and resource management affecting congestion [16,18]. The second assesses disruption losses and operational responses [7,9,24], while the third addresses alternative port selection, cargo allocation, and predefined rerouting scenarios [8,12,14]. However, the reviewed studies have not sufficiently addressed when diversion decisions at each vessel arrival reduce total logistics cost, considering congestion at both ports and the additional waiting costs imposed on vessels originally bound for the alternative port.

Table 1. Comparison of related studies on port congestion, disruptions, and vessel diversion.

Study	Alternative Port Diversion	Queue-Based Vessel Diversion	Port Operations Simulation	Economic Cost Evaluation	Simulation-Based Policy Optimization
Port planning, terminal operations, and congestion					
Shabayek and Yeung (2002) [16]	X	X	O	X	X
Saeed and Larsen (2016) [18]	X	X	X	O	X
Port closures, disaster impacts, and resilience					
Zhang et al. (2020) [7]	X	X	X	O	X
Verschuur et al. (2020) [9]	O	X	X	X	X
Li et al. (2024) [24]	O	X	O	X	X
Alternative port planning and cargo rerouting					
Martagan et al. (2009) [14]	O	X	O	X	X
Akakura et al. (2015) [8]	O	X	X	O	X
Achurra-Gonzalez et al. (2019) [12]	O	X	X	O	X
This study	**O**	**O**	**O**	**O**	**O**

O: explicitly considered; X: not explicitly considered.

The contributions of this study are summarized as follows. First, we formulate a state-based diversion policy that determines vessel assignments using the observed queue at the primary port, diversion probability R, and available reception capacity at the alternative port. The policy accounts for vessels waiting at the alternative port and reserves reception capacity for diverted vessels en route, preventing multiple vessels from being assigned to the same capacity. Second, we formulate total logistics cost in terms of vessel assignments and the resulting queueing processes at both ports. The formulation includes the waiting and cargo time costs of vessels originally bound for the alternative port, allowing the benefits of congestion relief at the primary port to be evaluated against the additional costs generated by diversion. Third, we compare the selected policy with no diversion, fixed-share diversion, and an optimized deterministic threshold policy to examine when diversion reduces total logistics cost and whether allowing $0 < R < 1$ provides an additional cost reduction. We further estimate break-even cargo time values across closure durations and interport inland transportation costs to identify the economic conditions under which diversion becomes beneficial.

3. Research Methodology

3.1. Problem Definition

This study considers a port system consisting of a primary port and an alternative port. A disaster temporarily prevents new vessel service from starting at the primary port.

The two ports normally serve their respective vessels using separate berths and cargo handling facilities. Vessels arriving at the primary port can be diverted to the alternative port to reduce congestion.

Diverted vessels share the alternative port's berths with vessels originally bound for that port and incur additional sailing and transportation costs. Policy performance is evaluated using total logistics cost, considering vessels remaining at the primary port, diverted vessels, and vessels originally bound for the alternative port.

The model adopts the following assumptions. Both ports are modeled as multiple berth queueing systems with fixed berth capacities and a first in, first out (FIFO) service discipline. Vessel interarrival times follow exponential distributions, while service times are sampled from empirical distributions specific to each port. Each vessel originally bound for the primary port retains its sampled service time regardless of its assigned port.

The closure duration is fixed for each scenario. Temporary berthing restrictions may prevent new vessel berthing while allowing cargo handling on vessels already alongside when weather conditions permit [27]. The modeled closure suspends new berthing and service starts at the primary port. Vessels already in service are assumed to complete their operations [28]. The framework applies to coordinated diversion settings in which the alternative port and the diversion route remain operational.

Diversion decisions are made centrally using shared real-time operational information. Each vessel is assigned a destination upon arrival at the primary port, and the assigned destination is not subsequently changed.

3.2. State-Based Dynamic Diversion Policy

The diversion policy is defined by the queue threshold T and diversion probability R. When a vessel arrives at the primary port, it is eligible for diversion if the number of waiting vessels reaches or exceeds T and reception capacity is available at the alternative port. Otherwise, the vessel remains at the primary port. Each eligible vessel is diverted with probability R, determined by a Bernoulli trial.

When diversion is confirmed, reception capacity is reserved for the vessel during its additional sailing time. Upon arrival at the alternative port, the reservation becomes an internal waiting position and is released when service begins. If service begins immediately, the reservation is released directly. This reservation mechanism prevents the same reception capacity from being assigned to multiple vessels.

The queue threshold T and diversion probability R remain fixed within each simulation replication. The term "dynamic" refers to state-based vessel assignment: at each vessel arrival, the diversion decision is made using the current primary-port queue and the available reception capacity at the alternative port. The same diversion rule is applied before, during, and after the closure. This allows the policy to respond continuously to observed congestion, including queues that persist after reopening.

Figure 1 illustrates the vessel flows and diversion decisions in the proposed port system.

3.3. Simulation Model and Optimization Procedure

A DES model is developed to represent stochastic vessel arrivals, service times, and queueing processes at both ports. Simulation optimization is performed to identify the diversion policy with the lowest estimated mean total logistics cost among predefined candidate policies.

3.3.1. Sets, States, and Variables

Let S denote the set of vessels originally bound for the primary port during a simulation replication, and S^+ denote the subset arriving during the evaluation period after

warm-up. The set S is divided into vessels remaining at the primary port (M) and vessels diverted to the alternative port (A), where $S = M \cup A$ and $M \cap A = \varnothing$. Costs are evaluated for $M \cap S^+$ and $A \cap S^+$. Let O_A denote the set of vessels originally bound for the alternative port that arrive during the evaluation period.

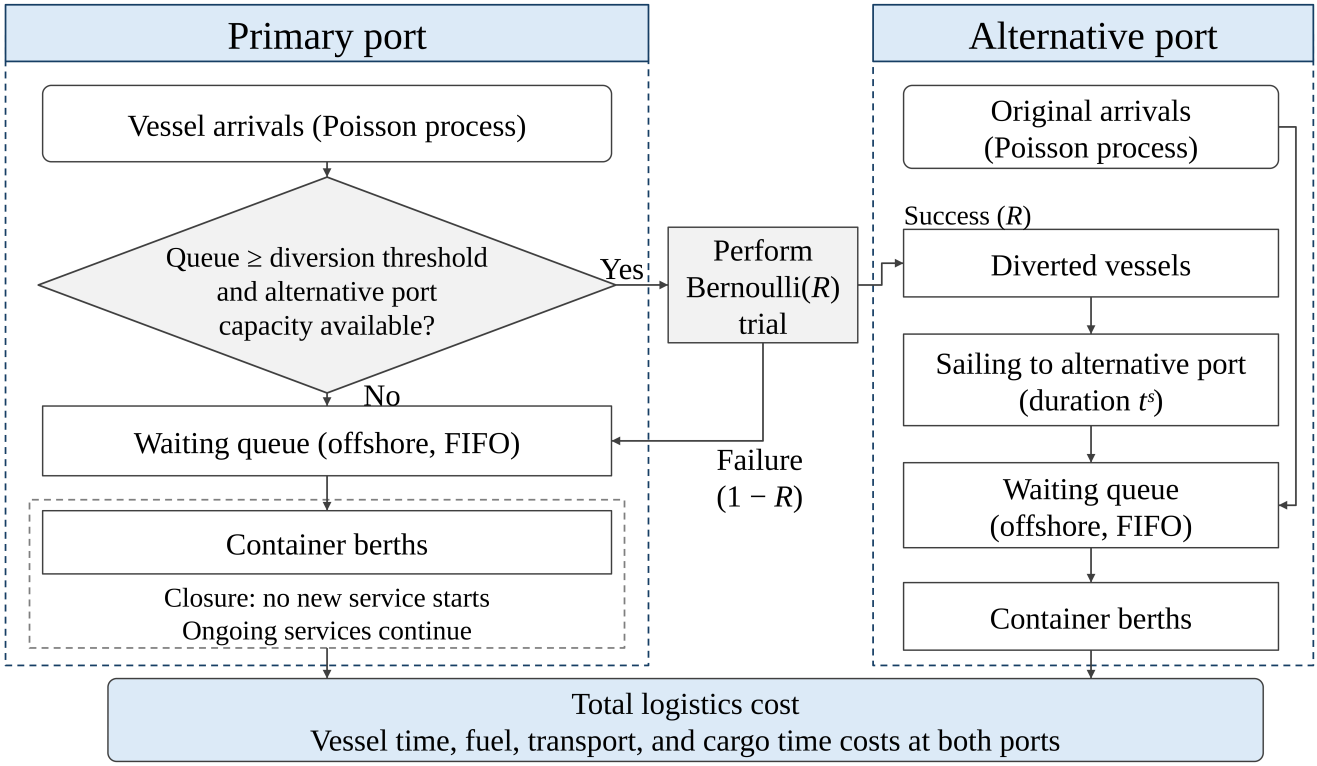


Figure 1. Simulation framework for dynamic vessel diversion.

For vessel i, a_i and b_i denote its initial arrival time and service start time, respectively. For a vessel originally bound for the primary port, a_i is also the diversion decision time. The binary indicator D_i equals one if the vessel is diverted and zero otherwise. Waiting times at the primary and alternative ports are denoted by w_i^M and w_i^A, respectively. The service time is denoted by s_i, and the additional sailing time is denoted by t^s.

Table 2 summarizes the notation used in the model.

Table 2. Definitions of the notation.

Symbol	Definition
S	Set of vessels originally bound for the primary port
S^+	Subset of S included in cost evaluation
M, A	Sets of vessels remaining at the primary port (M) and diverted to the alternative port (A)
O_A	Evaluated vessels originally bound for the alternative port
T, R	Queue threshold T and diversion probability R
$Q_M(t)$	Number of vessels waiting at the primary port at time t
$Q_A^{\text{in}}(t)$	Number of vessels in the alternative port's internal waiting area at time t
$E_A(t)$	Number of diverted vessels en route to the alternative port at time t
K	Reception capacity for internal waiting and reservations for vessels en route
D_i	Binary diversion indicator for vessel i
a_i, b_i	Initial arrival time a_i and service start time b_i for vessel i
w_i^M, w_i^A	Waiting times of vessel i at the primary and alternative ports, respectively
s_i	Service time of vessel i
t^s, t^r	Additional sailing time t^s and interport inland travel time t^r

Table 2. *Cont.*

Symbol	Definition
C^d	Vessel time cost per vessel-hour, excluding fuel
C^n, C^l	Interterminal transportation cost C^n and interport inland transportation cost C^l, per twenty-foot equivalent unit (TEU)
p_f	Fuel price per tonne
f_p, f_s	Hourly fuel consumption during waiting/service (f_p) and sailing (f_s)
V, V^e	Representative discharged volume V and export loading volume V^e per call
α	Share of discharged cargo requiring interterminal transportation at the primary port
β	Share of discharged cargo requiring return to the primary port for transshipment after diversion
γ	Interterminal transportation share within transshipment cargo, with $\alpha = \beta\gamma$
ϕ_m, ϕ_e, ϕ_t	Loaded-container shares of import (ϕ_m), export (ϕ_e), and transshipment (ϕ_t) cargo
L	Representative loaded cargo volume associated with a primary port vessel call
L_A	Representative loaded cargo volume associated with a vessel originally bound for the alternative port
h	Cargo time value (USD per loaded TEU-hour)
C^M, C^A, C^{O_A}	Cost components for evaluated vessels in M, A, and O_A, respectively
C^B, C^H	Cargo backlog cost C^B and other cargo time cost C^H
$TC(T, R)$	Total logistics cost under policy (T, R)
Θ, n	Set of candidate policies Θ and number of replications n
$\overline{TC}(T, R)$	Estimated mean total logistics cost under policy (T, R)
$\hat{s}(T, R)$	Sample standard deviation of replication costs under policy (T, R)
$H(T, R)$	Confidence interval half-width for mean cost under policy (T, R)
E	Confidence interval overlap set

3.3.2. Queue States and Diversion Rule

The number of vessels waiting at the primary port at time t is defined as

$$Q_M(t) = |\{i \in M : a_i \leq t < b_i\}|. \tag{1}$$

At the alternative port, reception capacity is occupied by vessels waiting internally and reservations for diverted vessels en route. The capacity constraint is

$$Q_A^{\text{in}}(t) + E_A(t) \leq K. \tag{2}$$

Vessels in service are excluded from this capacity limit. Vessels originally bound for the alternative port wait externally when internal waiting space is unavailable. Their external waiting time is included in cost evaluation.

Let B_i denote a Bernoulli random variable with success probability R. The diversion decision for vessel i is defined as

$$D_i = \begin{cases} B_i, & Q_M(a_i^-) \geq T, \\ & Q_A^{\text{in}}(a_i^-) + E_A(a_i^-) < K, \qquad B_i \sim \text{Bernoulli}(R). \\ 0, & \text{otherwise}, \end{cases} \tag{3}$$

Here, a_i^- denotes the system state immediately before the diversion decision. When events share the same timestamp, closure or reopening events are processed first, followed by service completions and then vessel arrivals. Arrivals sharing a timestamp are processed sequentially in scheduling order, with reception capacity reservations updated immediately when diversion is confirmed.

3.3.3. Waiting Times and Total Logistics Cost

For a vessel remaining at the primary port, waiting time is defined as $w_i^M = b_i - a_i$. For a diverted vessel, waiting time at the alternative port is $w_i^A = b_i - a_i - t^s$, excluding additional sailing time. For a vessel originally bound for the alternative port, waiting time is $w_j^A = b_j - a_j$, including any external waiting time.

All time quantities in the cost equations are expressed in hours, and all cost components are calculated in USD. Input durations reported in minutes are converted to hours, while daily vessel costs and fuel consumption rates are divided by 24 to obtain hourly values.

The cost of vessels remaining at the primary port consists of vessel time, fuel, and interterminal transportation costs:

$$C^M(T,R) = \sum_{i \in M \cap S^+} \Big[(C^d + p_f f_p)(w_i^M + s_i) + C^n \alpha V \Big]. \tag{4}$$

The parameter C^d represents hourly vessel cost excluding fuel, while $p_f f_p$ represents hourly fuel cost during waiting and service. The quantity αV represents the discharged cargo volume requiring interterminal transportation. The parameter α is calculated as $\alpha = \beta\gamma$, where β is the transshipment cargo share and γ is the interterminal transportation share within transshipment cargo.

The cost of diverted vessels includes waiting and service at the alternative port, additional sailing, and inland transportation between the two ports:

$$\begin{aligned} C^A(T,R) = \sum_{i \in A \cap S^+} \Big[& (C^d + p_f f_p)(w_i^A + s_i) \\ & + (C^d + p_f f_s) t^s + C^l(\beta V + V^e) \Big]. \end{aligned} \tag{5}$$

The quantity βV represents transshipment cargo discharged at the alternative port and returned to the primary port for onward shipping. The quantity V^e represents export cargo transferred from the primary port to the alternative port. The same transportation cost per TEU is applied to cargo moving in each direction. The fuel consumption rates f_p and f_s are expressed on an hourly basis.

The vessel time and fuel costs for vessels originally bound for the alternative port are calculated as

$$C^{O_A}(T,R) = \sum_{j \in O_A} (C^d + p_f f_p)(w_j^A + s_j). \tag{6}$$

This cost component accounts for the additional waiting burden imposed on vessels originally bound for the alternative port.

Cargo time costs are considered only for loaded containers. The representative loaded cargo volume associated with a primary port vessel call is defined as

$$L = V[(1-\beta)\phi_m + \beta\phi_t] + V^e\phi_e.$$

Here, ϕ_m, ϕ_e, and ϕ_t denote the shares of loaded import, export, and transshipment containers, respectively. The quantity L represents the cargo volume associated with a vessel call rather than the nominal vessel capacity. Transportation costs also include the movement of empty containers.

Cargo backlog cost is calculated for loaded cargo awaiting service at both ports. Let L_A denote the representative loaded cargo volume associated with a vessel originally bound for the alternative port:

$$C^B(T,R) = h\left[L\left(\sum_{i\in M\cap S^+} w_i^M + \sum_{i\in A\cap S^+} w_i^A\right) + L_A \sum_{j\in O_A} w_j^A\right]. \tag{7}$$

The parameter h represents cargo time value (USD per loaded TEU-hour) and is applied to all vessel groups within each cargo time value condition.

Other cargo time costs arise from vessel service at both ports, additional sailing, and inland transportation of diverted transshipment cargo:

$$C^H(T,R) = h\left[L\sum_{i\in S^+} s_i + L_A\sum_{j\in O_A} s_j + \sum_{i\in A\cap S^+} (Lt^s + \beta V\phi_t t^r)\right]. \tag{8}$$

Export cargo is assumed to be ready when diversion is decided. Inland transportation of export cargo occurs concurrently with the vessel's additional sailing and is completed before the vessel arrives at the alternative port. Therefore, its inland travel time is not added separately to cargo time costs. Transshipment cargo is returned to the primary port after service at the alternative port, and its inland travel time is included as an additional cost component. Interterminal travel time is excluded from cargo time costs.

Total logistics cost is calculated by combining the costs of the three vessel groups and cargo time costs:

$$TC(T,R) = C^M(T,R) + C^A(T,R) + C^{O_A}(T,R) + C^B(T,R) + C^H(T,R). \tag{9}$$

Under the same arrival and service samples, service costs that are independent of diversion decisions remain identical across policies within each replication and do not affect policy ranking.

Vessel time, fuel, and cargo time costs for vessels originally bound for the alternative port are included, but differences in inland transportation costs to the final destinations of import cargo are excluded. Therefore, total logistics cost represents the generalized cost within the defined evaluation scope.

3.3.4. Optimization and Statistical Evaluation

Simulation optimization determines decision variables by evaluating an objective function through simulation [29]. For each closure duration, the optimization problem is formulated as

$$\min_{(T,R)\in\Theta} \mathbb{E}[TC(T,R)], \tag{10}$$

where Θ denotes the predefined set of candidate diversion policies.

Let $TC_k(T,R)$ denote total logistics cost in replication k. The estimated mean cost over n replications is calculated as

$$\overline{TC}(T,R) = \frac{1}{n}\sum_{k=1}^{n} TC_k(T,R). \tag{11}$$

The policy (T^*, R^*) is selected as the combination with the lowest estimated mean total logistics cost in the selection sample among the predefined candidates in Θ. The term

optimal refers to this selection criterion and does not imply statistical superiority over the other candidates.

The half-width of the 95% confidence interval for mean total logistics cost is calculated as

$$H(T,R) = t_{0.975,n-1}\frac{\widehat{s}(T,R)}{\sqrt{n}}, \tag{12}$$

where $\widehat{s}(T,R)$ is the sample standard deviation of replication costs and $t_{0.975,n-1}$ is the 97.5th percentile of Student's t distribution with $n-1$ degrees of freedom. The confidence interval is

$$\left[\overline{TC}(T,R) - H(T,R), \overline{TC}(T,R) + H(T,R)\right].$$

The confidence interval overlap set (CIOS) comprises candidate policies whose individual confidence intervals for mean cost overlap that of the selected policy:

$$E = \Big\{(T,R) \in \Theta : \overline{TC}(T,R) - H(T,R) \leq \overline{TC}(T^*,R^*) + H(T^*,R^*)\Big\}. \tag{13}$$

The CIOS provides a descriptive summary of individual confidence interval overlap across the parameter grid. Inclusion in the set does not establish statistical equivalence between policies or determine the statistical significance of their mean cost differences.

4. Simulation Experiments and Results

4.1. Model Parameters

In this study, Busan Port is designated as the primary port subject to temporary closure, while Gwangyang Port is designated as the alternative port. The numbers of berths at Busan and Gwangyang are set to 34 and 8, respectively. The reception capacity of Gwangyang is set to $K = 13$ based on its reported anchorage capacity [30]. This limit includes vessels waiting internally and reservations for diverted vessels en route.

Vessel arrival and service data are obtained from the 2024 Port Management Information System (PORT-MIS) records for fully cellular container vessels [31]. Interarrival times follow exponential distributions, while service times are sampled from empirical distributions constructed for each port. To construct the empirical service-time distributions, port stays shorter than 300 min and those exceeding the upper IQR-based outlier threshold are excluded. The Container Port Performance Index 2023 reports that cargo operations and berth idle time account for 59.4% and 11.7% of total port time, respectively, in its global sample [32]. Their combined share of 71.1% provides the basis for applying a factor of 0.70 to the retained port-stay durations to approximate berth occupancy. Waiting before service is calculated separately within the queueing model. Vessels diverted from Busan to Gwangyang retain their sampled service times.

Figure 2 compares the observed interarrival-time quantiles at Busan and Gwangyang with theoretical exponential quantiles based on the mean interarrival times used in the model. The plots show close agreement over much of the distribution, with deviations in the upper tail. Quarterly differences in interarrival times are examined using the Kruskal–Wallis test. No statistically significant differences are detected at the 5% significance level for either port (Busan: $p = 0.5205$; Gwangyang: $p = 0.2287$).

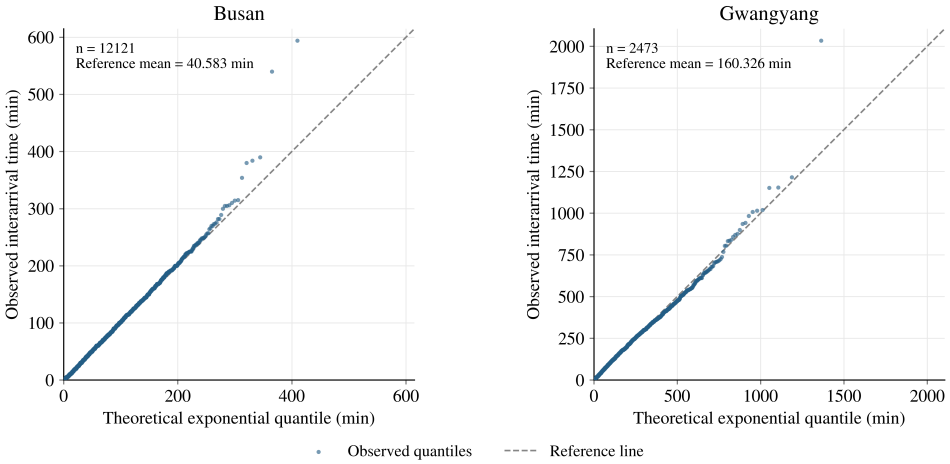


Figure 2. Q–Q plots of vessel interarrival times at Busan and Gwangyang.

Table 3 summarizes the port operating parameters.

Table 3. Port operating parameters.

Parameter	Busan	Gwangyang
Number of berths	34	8
Mean interarrival time (min)	40.583	160.326
Interarrival-time distribution	Exponential	Exponential
Service-time sample size	12,122	2474
Mean service time (min)	926.947	408.627
Service-time distribution	Empirical	Empirical
Reception capacity K (vessels) [30]	Unrestricted	13

Cargo composition is determined using the official container throughput statistics for Busan Port in 2024 [33]. Total throughput was 24,402,020 TEU, including 13,497,184 TEU of transshipment cargo. The transshipment share of total throughput is set to $\beta = 0.5531$. The representative discharged cargo volume is set to $V = 931.5$ TEU per call, and export loading volume is assumed to be equal to the discharged volume ($V^e = 931.5$).

According to Busan Port Authority, approximately 40% of transshipment cargo requires transportation between terminals [34]. This proportion is applied as $\gamma = 0.40$, giving $\alpha = \beta\gamma = 0.2212$ for the interterminal transportation share of the discharged cargo volume. Using the loaded-container shares obtained from the throughput statistics, the representative loaded cargo volume is calculated as $L = 1480.22$ TEU per call.

For vessels originally destined for Gwangyang, the representative loaded cargo volume is calculated as $L_A = 458.79$ TEU per call using the 2024 loaded container throughput of 1,508,027 TEU [33] and 3287 vessel calls recorded before service-time filtering.

Historical monetary inputs are adjusted to August 2026 prices using the Korean consumer price index (CPI) [35]. Annual CPI growth factors are applied from the year following each input's reference year through 2025, followed by the ratio of the August 2026 index (120.05) to the 2025 annual average (116.61). The reference years are 2011 for vessel costs, 2020 for fuel prices, 2018 for interterminal transportation costs, and 2022 for cargo time values. Fixed exchange rates of 1500 KRW/USD and 6.35 CNY/USD are used for interport inland transportation charges and cargo time values, respectively. Cargo time values are converted to USD before CPI adjustment. The 2026 interport inland transportation charge is not further adjusted.

Vessel costs and fuel consumption rates are obtained from a representative vessel benchmark with a capacity of approximately 4800 TEU [36]. The reference vessel cost is

USD 21,000 per day, with fuel consumption rates of 5.3 tonnes per day during waiting and service and 57.4 tonnes per day during sailing at 16 knots. A reference fuel price of USD 570 per tonne is adopted from Zhao et al. [37]. These monetary values are adjusted using the CPI.

The interport inland transportation charge is set to KRW 668,700 per 40-foot container based on the government freight rate schedule [38]. Using an exchange rate of 1500 KRW/USD and two TEU per 40-foot container, the corresponding cost is C^l = USD 222.90/TEU. For interterminal transportation, USD 25 per container is adopted as a proxy for transportation cost [39], converted to a per-TEU rate assuming two TEU per container and adjusted using the CPI.

Cargo time values are based on published estimates for nine export commodity categories in China's Yangtze River Delta [40]. The minimum, median, and maximum values of CNY 5.9, 14.9, and 39.2/TEU-hour are adopted for the low, medium, and high conditions, respectively. After currency conversion and CPI adjustment to August 2026 prices, the corresponding cargo time values are h = USD 1.035061, 2.613967, and 6.877013 per loaded TEU-hour. A common cargo time value is applied to the representative loaded cargo within each condition.

Additional sailing time is set to $t^s = 6.4375$ h based on a distance of 103 nautical miles and a sailing speed of 16 knots. Interport inland travel time is assumed to be $t^r = 4$ h. These values are treated as experimental parameters rather than observed travel times.

Table 4 presents the cost and cargo parameters.

Table 4. Cost and cargo parameters.

Parameter	Value	Unit and Basis
C^d	1168.91	USD/vessel-hour; CPI-adjusted vessel benchmark [36]
p_f	684.05	USD/tonne; CPI-adjusted reference price [37]
f_p	5.3/24	Tonnes/hour during waiting and service [36]
f_s	57.4/24	Tonnes/hour during sailing at 16 knots [36]
C^n	15.1364	USD/TEU; CPI-adjusted transportation revenue proxy [39]
C^l	222.90	USD/TEU; conversion of the adopted freight-rate input [38]
Exchange rate	1500	KRW/USD; conversion assumption
V	931.5	TEU/call; representative discharged volume
V^e	931.5	TEU/call; assumed equal to V
β	0.5531	Transshipment share based on port throughput [33]
γ	0.40	Interterminal share within transshipment cargo [34]
α	0.2212	Interterminal share of discharged cargo; $\beta\gamma$
ϕ_m	0.5897	Loaded-container share of imports [33]
ϕ_e	0.8035	Loaded-container share of exports [33]
ϕ_t	0.9438	Loaded-container share of transshipment cargo [33]
L	1480.22	Loaded TEU/call; calculated from cargo composition
L_A	458.79	Loaded TEU/call; Gwangyang loaded throughput per vessel call [33]
t^s	6.4375	Hours; specified distance divided by sailing speed
t^r	4	Hours; inland travel-time assumption
h	1.04, 2.61, 6.88	USD/loaded TEU-hour; low, medium, and high sensitivity inputs [40]

4.2. Experimental Design

The DES model is implemented in Python 3.12.10 using SimPy 4.1.2 and NumPy 2.5.1 for random number generation.

Eight closure durations are considered: 12, 24, 36, 48, 60, 72, 84, and 96 h. Each replication begins with 100 h of port operations before closure to establish the initial queue and berth occupancy conditions. Closure begins at hour 100, and vessel arrivals are generated until hour 600. Total logistics costs are evaluated for vessels arriving during the

500 h period from hours 100 to 600, including their waiting and service times beyond the arrival window.

The candidate diversion policies are defined as

$$T \in \{0, 5, 10, \ldots, 100\}, \qquad R \in \{0, 0.1, 0.2, \ldots, 1.0\}.$$

The 231 parameter combinations include 21 identical no-diversion policies with $R = 0$, resulting in 211 distinct candidate policies for each closure duration.

Policy parameters are selected separately for each closure duration, while the diversion rule uses the observed queue length and reception capacity without directly considering the remaining closure duration.

The 211 candidate policies are evaluated for each of the eight closure durations using 300 selection replications per policy, yielding 506,400 simulation runs. Vessel-level inputs are generated once per replication and reused across candidate policies and closure durations using common random numbers. DES outcomes are used to calculate total logistics costs under the three cargo time value conditions. For each condition, grid search selects the policy with the lowest mean total logistics cost. CIOSs are constructed from the selection sample using Equation (13).

The selected policies are subsequently evaluated using 300 independent replications. Common random numbers are applied across policies to obtain paired cost comparisons. Reported performance estimates and confidence intervals are based on this independent evaluation sample. Cost and operating sensitivity analyses follow the same procedure, with policies reselected from the original 211 candidates under each condition. Separate random number streams are used for arrivals and service times at each port and for diversion decisions. Replication-specific seeds are fixed in advance, with independent seed sets for policy selection and evaluation.

The no-diversion policy is defined by $R = 0$. The percentage cost saving relative to no diversion is calculated as

$$\text{Saving}(T, R) = \frac{\overline{TC}_0 - \overline{TC}(T, R)}{\overline{TC}_0} \times 100,$$

where $\overline{TC}_0$ denotes the estimated mean total logistics cost without diversion.

The 100 h warm-up period is assessed against alternative periods of 50 and 200 h for the 96 h closure. Each condition uses 300 replications with fixed policies and matched arrival and service inputs from the onset of closure. The resulting mean total logistics costs and monetary savings are nearly identical across the three warm-up periods. The evaluation arrival window is also extended from 500 to 700 h using fixed policies and matched inputs over the common period. The corresponding changes in mean monetary savings are 0.000%, −0.011%, and −0.098% for the low, medium, and high cargo time value conditions, respectively.

An additional resolution check refines the selected policies with $R > 0$ using unit increments in T within five vessels of the selected threshold and increments of 0.05 in R within 0.1 of the selected probability, subject to $T \geq 0$ and $0 \leq R \leq 1$. Thresholds selected from the original $R = 1$ subset are also refined using unit increments within five vessels, bounded by $[0, 100]$. For selected policies with $R > 0$ and $T = 100$, additional thresholds from 105 to 150 in increments of five are evaluated. Every threshold in the expanded set is also evaluated at $R = 1$. For each closure duration, the additional candidates are pooled across the three cargo time value conditions and evaluated using the selection sample. The resulting policies are evaluated using 300 independent replications. The main analysis retains the original 211 candidates.

4.3. Policy Performance Across Closure Durations

Table 5 presents the selected diversion policies, mean total logistics costs, cost savings, and CIOSs under the three cargo time value conditions. No diversion is selected for all three conditions at 12 h, while diversion becomes more economically beneficial as closure duration increases.

Table 5. Selected diversion policies and cost performance (costs in USD million).

Duration (h)	T^*	R^*	No Diversion	Selected	Saving (%)	$\lvert E \rvert$	No Diversion in E
Low cargo time value							
12	N/A	0.0	37.5647	37.5647	0.0000	175	Yes
24	N/A	0.0	38.9263	38.9263	0.0000	140	Yes
36	N/A	0.0	42.1821	42.1821	0.0000	115	Yes
48	N/A	0.0	47.3147	47.3147	0.0000	94	Yes
60	100	0.5	54.3217	54.3263	−0.0086	87	Yes
72	80	0.2	63.2329	63.0958	0.2168	116	Yes
84	80	0.3	74.0384	73.0835	1.2897	152	Yes
96	70	0.6	86.6557	83.8716	3.2128	185	No
Medium cargo time value							
12	N/A	0.0	65.5114	65.5114	0.0000	179	Yes
24	N/A	0.0	67.9888	67.9888	0.0000	152	Yes
36	65	0.3	73.9125	73.9127	−0.0004	139	Yes
48	45	0.2	83.2510	83.0385	0.2553	146	Yes
60	40	0.3	95.9997	94.1419	1.9353	190	No
72	35	0.9	112.2133	106.4525	5.1338	128	No
84	15	1.0	131.8732	120.0772	8.9450	104	No
96	10	1.0	154.8297	135.0082	12.8021	75	No
High cargo time value							
12	N/A	0.0	140.9676	140.9676	0.0000	187	Yes
24	45	0.9	146.4574	146.4429	0.0099	170	Yes
36	20	0.3	159.5845	158.1746	0.8835	180	Yes
48	10	1.0	180.2791	173.0773	3.9948	68	No
60	5	1.0	208.5305	191.0638	8.3761	53	No
72	5	1.0	244.4603	212.4250	13.1045	38	No
84	5	1.0	288.0271	237.6979	17.4738	33	No
96	5	1.0	338.8994	266.8426	21.2620	29	No

Figure 3 compares the selected policies with no diversion. The left panels show mean total logistics costs with 95% confidence intervals, while the right panels show percentage cost savings.

Under the low cargo time value condition, no diversion is selected for closures of 12 to 48 h. At 60 h, the selected policy yields no mean cost reduction in independent evaluation. At 96 h, the selected policy $(T, R) = (70, 0.6)$ reduces mean total logistics cost by 3.21%.

Under the medium condition, diversion is selected from 36 h, but independent evaluation yields no mean cost reduction at that duration. The selected threshold decreases as closure duration increases, reaching $(10, 1.0)$ at 96 h with a cost saving of 12.80%. Under the high condition, the selected policy is $(5, 1.0)$ for closures of 60 to 96 h, yielding a saving of 21.26% at 96 h. These results indicate that higher cargo time values favor diversion at lower queue thresholds during longer closures.

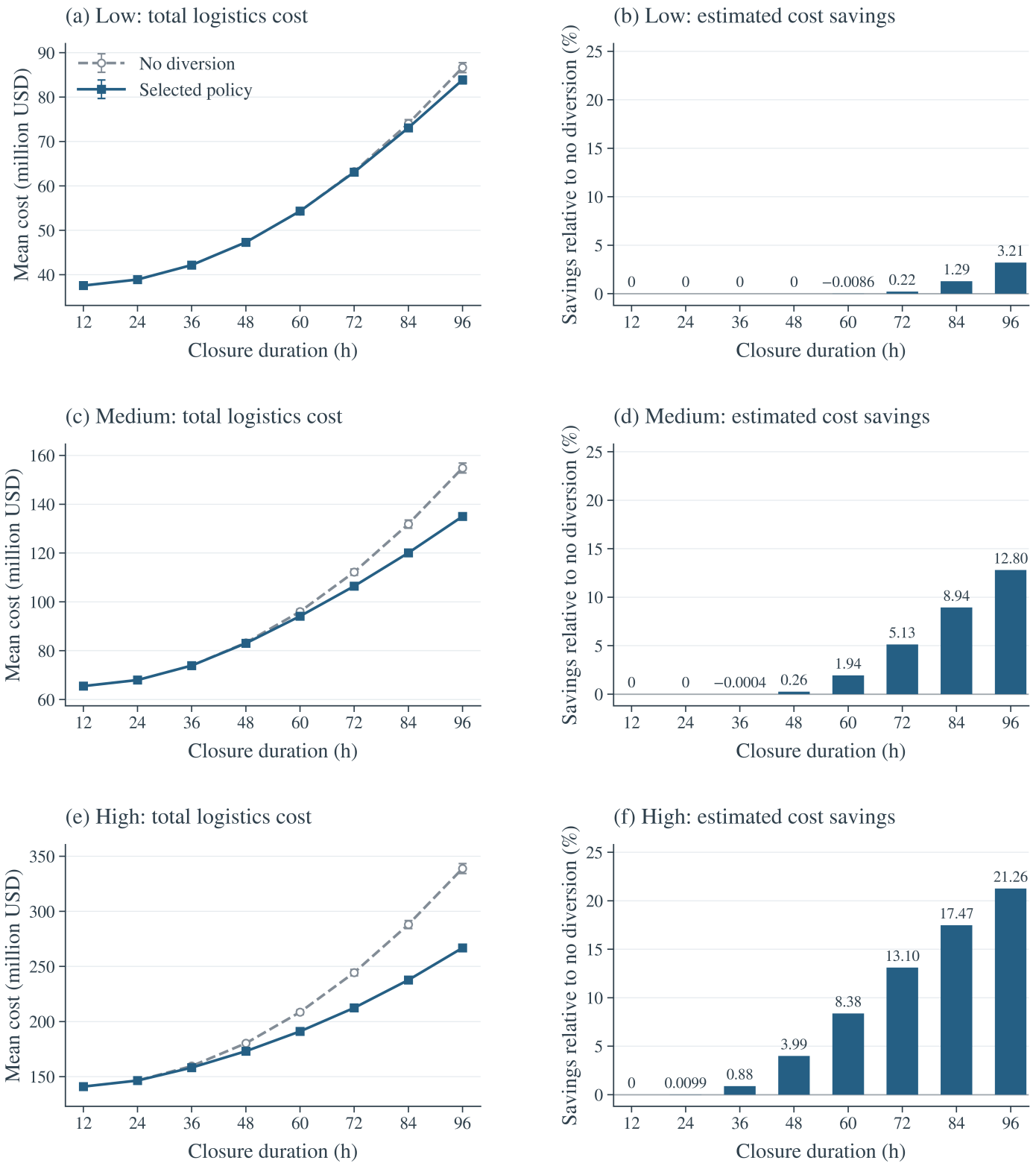


Figure 3. Total logistics costs and savings across closure durations.

Figure 4 presents the CIOSs for the 96 h closure under the low, medium, and high cargo time value conditions. Filled circles indicate policies included in the CIOS, open circles indicate excluded policies, and stars identify the selected policies. CIOS sizes for all closure durations are reported in Table 5.

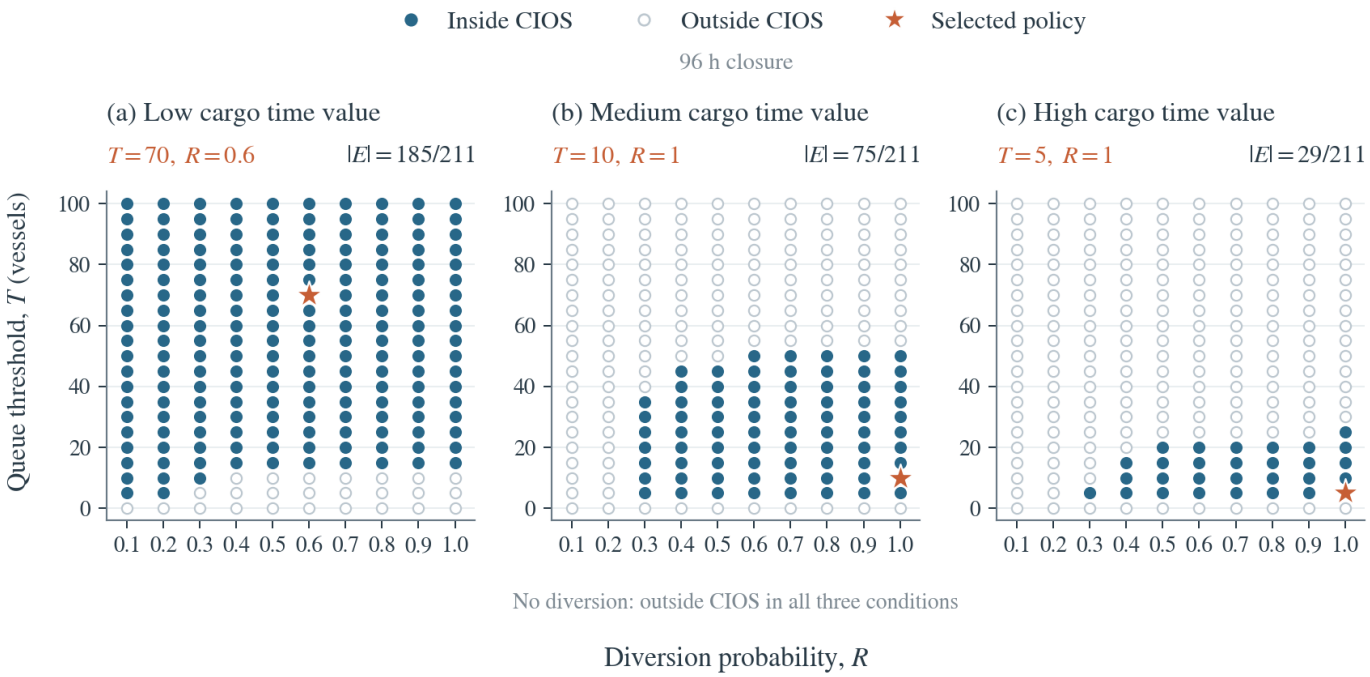


Figure 4. Confidence interval overlap sets for a 96 h closure under three cargo time value conditions.

At 96 h, the CIOS contains 185, 75, and 29 of the 211 candidates under the low, medium, and high conditions, respectively. Under the low condition, the CIOS spans a broad range of queue thresholds and diversion probabilities. Under the medium and high conditions, the included policies are concentrated at lower queue thresholds. Across the closure durations reported in Table 5, no diversion remains in the CIOS through 84 h under the low condition, 48 h under the medium condition, and 36 h under the high condition.

For the 96 h closure under the low condition, independent evaluation estimates a mean cost reduction of USD 2.784 million relative to no diversion, with a Bonferroni-adjusted 95% confidence interval of USD 2.410–3.158 million.

The estimated benefits are much smaller in some shorter-closure cases. Under the high condition at 24 h, mean savings are 0.0099%, corresponding to USD 14,483, with a 95% confidence interval from USD −6617 to USD 35,583.

Table 6 compares the original-grid selections with those from the expanded set of 309 candidates for the 96 h closure.

Table 6. Selected policies and independently evaluated mean percentage cost savings in the resolution check for a 96 h closure.

Cargo Time Value	Original Grid (211)		Expanded Set (309)	
	(T, R)	Saving (%)	(T, R)	Saving (%)
Low	$(70, 0.6)$	3.2128	$(71, 1)$	3.1637
Medium	$(10, 1)$	12.8021	$(9, 1)$	12.7899
High	$(5, 1)$	21.2620	$(2, 1)$	21.3401

Across the three conditions, the largest absolute difference in the saving rates is 0.0781 percentage points.

For the 60 h closure under the low condition, the original selection $(100, 0.5)$ lies at the upper threshold boundary. Extending the search to $T = 150$ produces an expanded set of 408 candidates and selects $(105, 1)$, but this policy does not reduce mean cost relative to no diversion in independent evaluation.

4.4. Cost Components and Operational Effects

Table 7 presents the cost components for the 96 h closure. Under the low cargo time value condition, diversion incurs an additional interport inland transportation cost of USD 11.201 million, while vessel time and cargo backlog costs decrease by USD 5.656 million and USD 8.234 million, respectively.

Table 7. Mean logistics cost components for the 96 h closure (USD million).

Component	Low		Medium		High	
	No Diversion	Selected	No Diversion	Selected	No Diversion	Selected
Vessel time	35.121	29.464	35.121	26.349	35.121	26.173
Fuel	4.539	4.140	4.539	4.030	4.539	4.036
Interport inland transportation	0.000	11.201	0.000	21.075	0.000	22.047
Interterminal transportation	2.305	2.196	2.305	2.101	2.305	2.091
Cargo backlog	26.568	18.334	67.095	33.723	176.519	86.685
Other cargo time	18.124	18.536	45.771	47.731	120.416	125.811
Total	86.656	83.872	154.830	135.008	338.899	266.843

Under the medium and high conditions, cargo backlog cost reductions are USD 33.372 million and USD 89.834 million, while additional interport inland transportation costs are USD 21.075 million and USD 22.047 million. The resulting net savings are USD 19.822 million and USD 72.057 million, respectively.

Figure 5 shows changes in cost components relative to no diversion for closures of 48 to 96 h. Negative values indicate cost reductions. The results show that reductions in cargo backlog costs increasingly offset additional transportation costs as closure duration increases.

Table 8 presents the operational effects of the selected policies for the 96 h closure.

Table 8. Mean operational indicators for the 96 h closure.

Indicator	No Diversion	Low	Medium	High
Evaluated arrivals at the primary port (vessels)	738.79	738.79	738.79	738.79
Diverted vessels	0.00	34.73	65.35	68.37
Maximum queue at the primary port (vessels)	141.60	115.44	99.79	98.68
Time from reopening until the last retained vessel arriving during the closure starts service (h)	55.11	42.99	36.02	35.48
Total waiting time of vessels originally bound for the alternative port (vessel-hours)	0.83	452.18	1015.41	1058.73
Maximum occupied reception capacity at the alternative port (vessels)	0.61	12.97	13.00	13.00
Maximum external queue at the alternative port (vessels)	0.00	3.33	4.75	4.85

Under the low, medium, and high conditions, an average of 34.73, 65.35, and 68.37 vessels are diverted, representing 4.70%, 8.85%, and 9.25% of primary port arrivals, respectively. The corresponding reductions in the mean maximum primary port queue are 18.47%, 29.53%, and 30.31%. The time from reopening until the last retained vessel that arrived during the closure starts service decreases by 12.12, 19.09, and 19.63 h, respectively.

Total waiting time for vessels originally bound for the alternative port increases from 0.83 vessel-hours without diversion to 452.18, 1015.41, and 1058.73 vessel-hours under the low, medium, and high conditions, respectively. The corresponding mean maximum reception occupancy is 12.97, 13.00, and 13.00 vessels, against a limit of 13 vessels. These results indicate that congestion reduction at the primary port should be evaluated together with additional waiting and logistics costs at the alternative port.

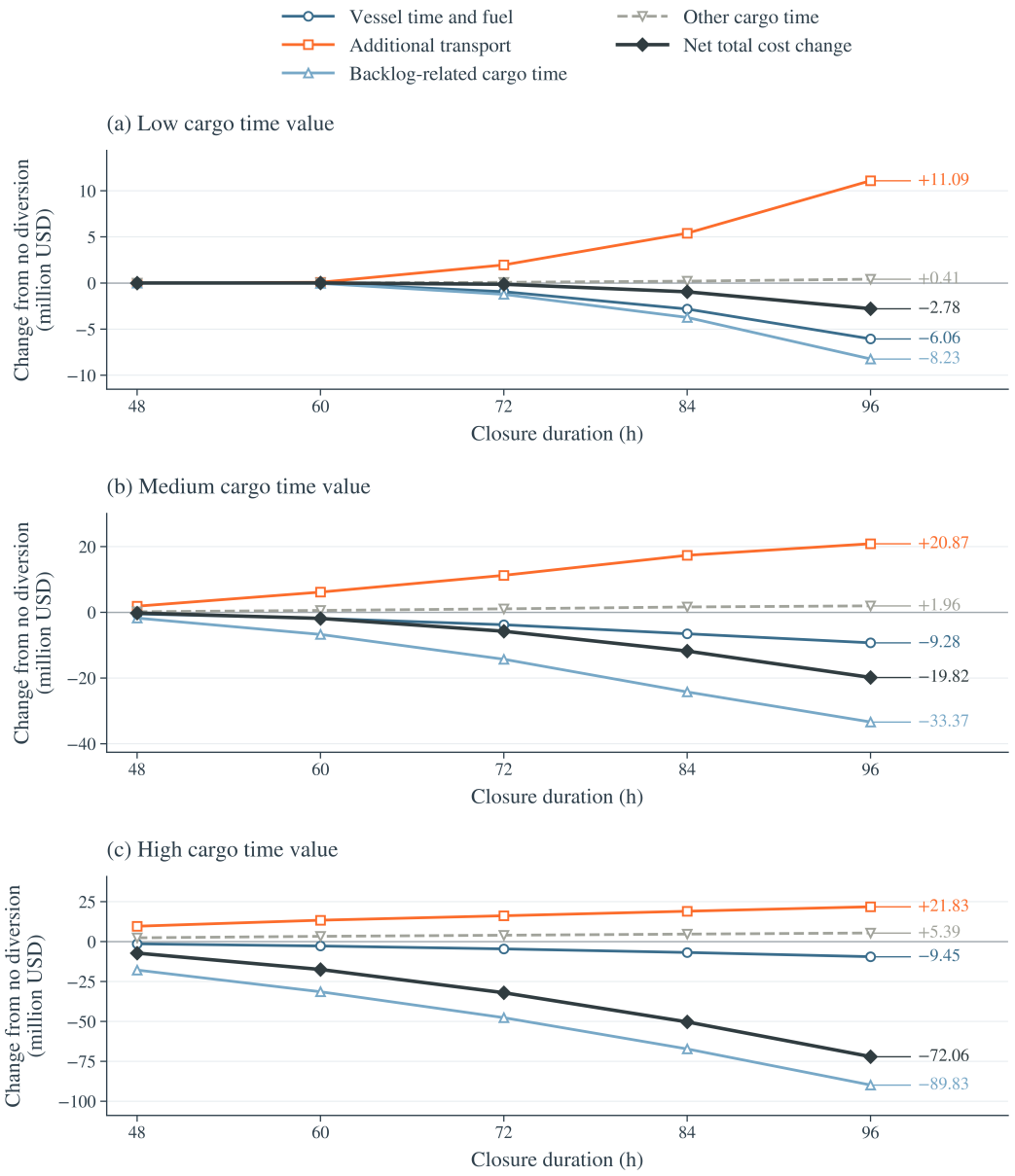


Figure 5. Changes in cost components relative to no diversion.

4.5. Comparison with Benchmark Policies

The selected diversion policy is compared with no diversion, fixed-share diversion, and a deterministic threshold policy. For fixed-share diversion, primary-port arrivals are counted when immediate service is unavailable due to port closure, existing queues, or full berth occupancy. The target diversion share is set to $8/(34 + 8) = 19.05\%$ based on the berth capacities of the two ports. The 6th, 11th, 16th, and 21st vessels in each group of 21 counted arrivals are selected for diversion, subject to available reception capacity. If capacity is unavailable, the vessel remains at the primary port. The counting sequence continues across closure and reopening.

The deterministic threshold policy fixes $R = 1$ and selects T from $\{0, 5, \ldots, 100\}$ using the original 300 selection replications for each closure duration and cargo time value, with no diversion included as an additional option. All policies are applied from the beginning of each replication and evaluated using the same 300 independent replications. Paired comparisons between the selected policy and the three benchmarks use Bonferroni-adjusted confidence intervals with a familywise confidence level of 95%.

Table 9 compares the policies for 48 and 96 h closures under the baseline operating and cost assumptions. The selected policies are obtained from the original 211 candidates. Savings are calculated relative to no diversion using the independent evaluation sample.

Table 9. Independently evaluated mean percentage cost savings relative to no diversion.

Closure (h)	Cargo Time Value	No Diversion	Fixed Share 19.05%	Deterministic Threshold	Selected Policy
48	Low	0.0000	−10.5042	0.0000	0.0000
48	Medium	0.0000	−2.5181	0.1378	0.2553
48	High	0.0000	3.1410	3.9948	3.9948
96	Low	0.0000	1.1370	3.1626	3.2128
96	Medium	0.0000	10.7932	12.8021	12.8021
96	High	0.0000	17.4597	21.2620	21.2620

For the 48 h closure, fixed-share diversion increases mean total logistics cost under the low and medium cargo time value conditions and reduces it under the high condition. For the 96 h closure, all three diversion policies yield positive mean savings under all three conditions. The selected policies have lower mean costs than fixed-share diversion in all six reported conditions.

Under the 48 h medium cargo time value condition, the selected policy $(T, R) = (45, 0.2)$ reduces mean cost by USD 97,828 relative to the optimized deterministic threshold policy $(70, 1)$, with a Bonferroni-adjusted 95% confidence interval of USD 28,682–166,975. This is the only statistically significant improvement over that benchmark among the six reported conditions. Under the 96 h low condition, the estimated mean reduction for $(70, 0.6)$ relative to the deterministic threshold policy $(75, 1)$ is USD 43,506, but the corresponding interval, USD −28,838–115,850, includes zero. Both policies coincide with no diversion under the 48 h low condition. Under the 48 h high and 96 h medium and high conditions, both policies select the same threshold with $R = 1$ and therefore coincide.

For the 96 h closure, the selected policies reduce mean total logistics cost relative to fixed-share diversion by USD 1.799 million, USD 3.110 million, and USD 12.886 million under the low, medium, and high conditions, respectively. The corresponding Bonferroni-adjusted 95% confidence intervals are USD 1.638–1.960 million, USD 2.770–3.451 million, and USD 12.211–13.561 million. Under the low condition, fixed-share diversion diverts 55.30 vessels on average, compared with 34.73 under the selected policy. The corresponding mean maximum primary-port queues are 115.03 and 115.44 vessels, respectively, while fixed-share diversion incurs USD 6.633 million more interport inland transportation cost. Mean waiting times for vessels originally bound for the alternative port are 0.65 and 2.42 h, respectively.

4.6. Sensitivity to Cargo Time Value and Transportation Cost

Sensitivity analysis examines the joint effects of cargo time value h and interport inland transportation unit cost C^I. The low, medium, and high cargo time value conditions are combined with transportation unit costs of USD 178.32, 222.90, and 267.48/TEU, corresponding to 80%, 100%, and 120% of the baseline value. All other inputs are held at their baseline values within each closure-duration scenario.

Costs are recalculated from the selection records for each cost combination before policy reselection. Table 10 presents the selected policies and mean percentage cost savings for 48 and 96 h closures, relative to no diversion under the same cost assumptions.

Table 10. Selected policies and mean percentage cost savings under cargo time value and transportation cost scenarios.

Closure	C^l	Low		Medium		High	
(h)	(USD/TEU)	(T, R)	Saving (%)	(T, R)	Saving (%)	(T, R)	Saving (%)
48	178.32	$(85, 1)$	−0.0055	$(35, 0.3)$	0.8960	$(10, 1)$	5.0844
48	222.90	ND	0.0000	$(45, 0.2)$	0.2553	$(10, 1)$	3.9948
48	267.48	ND	0.0000	$(75, 0.8)$	0.0243	$(15, 1)$	2.9755
96	178.32	$(40, 1)$	6.0070	$(5, 1)$	15.2075	$(5, 1)$	22.1394
96	222.90	$(70, 0.6)$	3.2128	$(10, 1)$	12.8021	$(5, 1)$	21.2620
96	267.48	$(95, 0.3)$	1.1182	$(15, 1)$	9.6727	$(5, 1)$	19.5594

ND denotes no diversion ($R = 0$).

For the 96 h closure under the low cargo time value condition, reducing the transportation unit cost selects $(T, R) = (40, 1)$ with mean savings of 6.0070%, whereas increasing it selects $(95, 0.3)$ with savings of 1.1182%. Under the high condition, $(5, 1)$ is selected at all three transportation cost levels, with savings ranging from 19.5594% to 22.1394%.

For the 48 h closure, the low condition yields zero or slightly negative mean savings, including −0.0055% under the reduced transportation cost. Under the medium condition, increasing the transportation cost reduces mean savings to 0.0243%. These cases provide little estimated cost benefit from diversion. The results show that the selected policy and the magnitude of cost savings depend jointly on closure duration, cargo time value, and interport inland transportation unit cost.

To complement the comparison under the literature-based low, medium, and high cargo time values, a break-even analysis varies h continuously over USD 0–100 per loaded TEU-hour. For each closure duration and interport inland transportation unit cost C^l, mean total logistics costs are recalculated from the 300-replication selection records, and the policy with the lowest estimated mean total logistics cost is reselected from the original 211 candidates, including no diversion, at each h. The estimated break-even cargo time value is defined as the lower boundary of values at which a diversion policy has a lower selection-sample mean total logistics cost than no diversion. These boundaries are calculated from intersections of the mean total logistics cost functions of the candidate policies.

Table 11 presents the estimated break-even cargo time values across closure durations and interport inland transportation unit costs.

Table 11. Estimated break-even cargo time values.

Closure	Interport Inland Transportation Unit Cost C^l (USD/TEU)			Selected
(h)	178.32	222.90	267.48	(T, R)
12	44.23	55.30	66.38	$(25, 0.5)$
24	2.85	3.77	4.69	$(50, 0.8)$
36	1.60	2.21	2.82	$(70, 0.9)$
48	0.71	1.10	1.49	$(90, 1.0)$
60	0.65	1.03	1.41	$(100, 0.5)$
72	0.46	0.80	1.13	$(100, 0.1)$
84	0.29	0.58	0.87	$(100, 0.1)$
96	0.17	0.43	0.69	$(100, 0.1)$

Values are selection-sample estimates of the break-even cargo time value in USD per loaded TEU-hour. The reported (T, R) is selected immediately above the boundary at C^l = USD 222.90/TEU and may change as h increases. Results use the original 211 candidates; the policies at 60–96 h reach the upper threshold limit $T = 100$.

The estimated break-even cargo time value decreases with closure duration and increases with interport inland transportation unit cost. At the baseline value of

C^l = USD 222.90/TEU, the estimate decreases from 55.30 for a 12 h closure to USD 0.43 per loaded TEU-hour for a 96 h closure. The 12 h estimate exceeds all three literature-based cargo time values, consistent with no diversion being selected under those conditions. These estimates are subject to sampling uncertainty in the selection records. Independent evaluation yields paired 95% confidence intervals for mean cost differences that include zero at the estimated boundaries, indicating uncertainty in the cost advantage of diversion there. The estimates apply under the baseline arrival, service-time, and capacity conditions to closures of specified duration that suspend new service starts at the primary port while the alternative port and diversion route remain operational.

4.7. Sensitivity to Operating Conditions

Operating sensitivity analysis examines departures from the baseline assumptions that each diverted vessel retains its sampled service time and that eight berths are available at Gwangyang. Service-time multipliers of 0.8 and 1.2 are applied only to diverted Busan-bound vessels, representing symmetric decreases and increases of 20% relative to baseline. The six-berth scenario represents a 25% reduction in the number of available berths. These levels are specified as controlled sensitivity scenarios to examine service-time differences and partial berth availability. Each change is applied separately, with the remaining inputs held at their baseline values.

Table 12 reports mean percentage cost savings of the reselected policies relative to no diversion under each operating condition.

Table 12. Independently evaluated mean percentage cost savings under changes in diverted-vessel service time and available berth capacity.

Closure (h)	Operating Condition	Low	Medium	High
48	Baseline	0.0000	0.2553	3.9948
48	Diverted-vessel service × 0.8	0.0000	0.4512	5.4758
48	Diverted-vessel service × 1.2	0.0000	0.1094	2.9828
48	Gwangyang: six berths	0.0000	0.1232	2.4704
96	Baseline	3.2128	12.8021	21.2620
96	Diverted-vessel service × 0.8	4.1945	15.7754	25.2240
96	Diverted-vessel service × 1.2	2.3177	10.2157	17.8767
96	Gwangyang: six berths	1.7284	8.2061	14.8283

For the 96 h closure under the high cargo time value condition, the service-time multipliers of 0.8 and 1.2 yield mean savings of 25.2240% and 17.8767%, respectively, compared with 21.2620% at baseline. Reducing Gwangyang's available berths to six yields savings of 1.7284%, 8.2061%, and 14.8283% under the low, medium, and high conditions, respectively.

For the 48 h closure, the low cargo time value condition yields zero mean savings across the tested operating conditions.

Additional sensitivity analysis replaces the baseline service-time conversion factor of 0.70 with 0.613 and 0.818 at both ports, drawing on the berth-time shares across ship-size groups reported in the Container Port Performance Index 2023 [32]. Following the same policy reselection and independent evaluation procedure, mean savings for the 96 h closure range from 0.1471% to 12.5763% under the low condition, 8.5192% to 21.3671% under the medium condition, and 18.6009% to 28.0407% under the high condition. The magnitude of the estimated cost savings is sensitive to the service-time conversion assumption.

5. Conclusions

This study developed a simulation optimization framework for dynamic vessel diversion under port closure disruptions. A state-based diversion policy was proposed to determine vessel diversion based on the observed queue at the primary port, diversion probability, and available reception capacity at the alternative port. A DES model and grid search were used to evaluate candidate diversion policies and select the policy with the lowest estimated mean total logistics cost, considering vessel time, fuel, transportation, and cargo time costs.

The case study using data from Busan and Gwangyang Ports shows that vessel diversion is not always economically beneficial during short closures. The selected policy depends on closure duration and cargo time value. For a 96 h closure, the selected policies reduce mean total logistics cost by 3.21%, 12.80%, and 21.26% under the low, medium, and high cargo time value conditions, respectively. The mean maximum queue length at the primary port decreases by 18.47% to 30.31%, while the time from reopening until the last retained vessel arriving during the closure starts service decreases by 12.12 to 19.63 h. However, diversion incurs additional transportation costs and increases waiting times for vessels originally bound for the alternative port. These results indicate that diversion policies should consider the congestion and logistics costs of both ports.

The selected policies yield lower mean costs than fixed-share diversion in all six benchmark conditions. Relative to the optimized deterministic threshold policy, a statistically significant improvement is observed only for the 48 h medium cargo time value condition; in the remaining cases, the differences are not statistically significant or the policies coincide. The break-even analysis further shows that the cargo time value required for diversion to become economically beneficial decreases with closure duration and increases with interport inland transportation cost. At the baseline transportation cost, the estimated break-even cargo time value decreases from USD 55.30 per loaded TEU-hour for a 12 h closure to USD 0.43 per loaded TEU-hour for a 96 h closure.

For practical implementation, port authorities, terminal operators, and shipping companies can use the selected policy to coordinate vessel diversion. Local operating data, anticipated closure durations, and cargo time values can be used to select (T, R) in advance by comparing estimated mean total logistics costs. An optimized deterministic threshold policy can also be considered when probabilistic diversion does not provide a statistically significant additional cost reduction. During operation, the selected parameters remain fixed, and diversion eligibility is determined by the current primary-port queue and available reception capacity at the alternative port. Eligible vessels are diverted with probability R, with reception capacity reserved while they are en route.

Implementation requires estimates of closure duration, shared information on port queues and reception capacity, and prior agreements on vessel acceptance, berth access, and interport inland transportation. Reception capacity must also accommodate vessels originally bound for the alternative port. Errors in the estimated closure duration may affect the resulting cost savings.

The findings are limited to the specified closure durations, tested operating conditions, and an alternative port unaffected by the disruption. Although port records are used to specify the model inputs, validation against observed vessel waiting times or berth utilization could not be performed with the available data. The estimated cost savings are sensitive to the service-time conversion factor, which limits the generalizability of the reported cost reductions. The analysis also assumes a common cargo time value within each scenario and excludes certain cargo time and inland transportation costs. Future research may consider uncertain closure durations and heterogeneous vessels and cargo.

Author Contributions: Conceptualization, Y.H.C. and S.W.C.; methodology, Y.H.C., M.W., and S.W.C.; software, Y.H.C.; validation, Y.H.C., M.W., and S.W.C.; formal analysis, Y.H.C.; investigation, Y.H.C., M.W., and J.K.; data curation, Y.H.C. and J.K.; writing—original draft preparation, Y.H.C., M.W., and J.K.; writing—review and editing, Y.K., S.W.C., and S.O.; visualization, Y.H.C.; supervision, S.W.C.; project administration, Y.K., S.O., and S.W.C.; funding acquisition, Y.K. and S.O. All authors have read and agreed to the published version of the manuscript.

Funding: This work was supported by Korea Institute of Marine Science & Technology Promotion (KIMST) funded by the Korea Coast Guard (RS-2025-14322995).

Institutional Review Board Statement: Not applicable.

Informed Consent Statement: Not applicable.

Data Availability Statement: The data presented in this study are available on request from the corresponding author due to the terms of use of the data provider.

Acknowledgments: The authors would like to express our sincere gratitude to the anonymous reviewers whose comments and feedback helped improve the quality of this paper.

Conflicts of Interest: The authors declare no conflicts of interest.

References

1. United Nations Conference on Trade and Development. *Review of Maritime Transport 2023: Towards a Green and Just Transition*; United Nations: Geneva, Switzerland, 2023.
2. Verschuur, J.; Koks, E.; Hall, J. Ports' criticality in international trade and global supply-chains. *Nat. Commun.* **2022**, *13*, 4351.
3. Panayides, P.; Song, D.W. Port integration in global supply chains: Measures and implications for maritime logistics. *Int. J. Logist. Res. Appl.* **2009**, *12*, 133–145.
4. Cho, S.; Hong, J.; Lee, H.; Lee, W. Technological forecasting of port digitalization using patent analysis. *Marit. Econ. Logist.* **2026**, *28*, 473–496.
5. Woo, M.; Yoo, T.; Lee, Y.; Cho, S.; Jung, W.S.; Kim, J.; Park, J.; Nanda, A. Emerging technology forecasting for the VHF data exchange system in maritime wireless communication. *J. Mar. Sci. Technol.* **2026**, *31*, 349–359.
6. Verschuur, J.; Koks, E.; Li, S.; Hall, J. Multi-hazard risk to global port infrastructure and resulting trade and logistics losses. *Commun. Earth Environ.* **2023**, *4*, 5.
7. Zhang, Y.; Wei, K.; Shen, Z.; Bai, X.; Lu, X.; Guedes Soares, C. Economic impact of typhoon-induced wind disasters on port operations: A case study of ports in China. *Int. J. Disaster Risk Reduct.* **2020**, *50*, 101719.
8. Akakura, Y.; Ono, K.; Watanabe, T.; Kawamura, H. Estimation of alternative ports for container transport after large-scale disasters: Estimation method and application to Port-BCPs. *J. Integr. Disaster Risk Manag.* **2015**, *5*, 135–152.
9. Verschuur, J.; Koks, E.; Hall, J. Port disruptions due to natural disasters: Insights into port and logistics resilience. *Transp. Res. Part D Transp. Environ.* **2020**, *85*, 102393.
10. Gross, D.; Harris, C. *Fundamentals of Queueing Theory*, 3rd ed.; Wiley: New York, NY, USA, 1998.
11. Dragović, B.; Park, N.; Radmilović, Z. Ship-berth link performance evaluation: Simulation and analytical approaches. *Marit. Policy Manag.* **2006**, *33*, 281–299.
12. Achurra-Gonzalez, P.; Novati, M.; Foulser-Piggott, R.; Graham, D.; Bowman, G.; Bell, M.; Angeloudis, P. Modelling the impact of liner shipping network perturbations on container cargo routing: Southeast Asia to Europe application. *Accid. Anal. Prev.* **2019**, *123*, 399–410.
13. Wang, S.; Qu, X.; Yang, Y. Estimation of the perceived value of transit time for containerized cargoes. *Transp. Res. Part A Policy Pract.* **2015**, *78*, 298–308.
14. Martagan, T.; Eksioglu, B.; Eksioglu, S.; Greenwood, A. A simulation model of port operations during crisis conditions. In Proceedings of the 2009 Winter Simulation Conference, Austin, TX, USA, 13–16 December 2009; pp. 2832–2843. https://doi.org/10.1109/WSC.2009.5429245.
15. Rose, A.; Wei, D. Estimating the economic consequences of a port shutdown: The special role of resilience. *Econ. Syst. Res.* **2013**, *25*, 212–232.
16. Shabayek, A.; Yeung, W. A simulation model for the Kwai Chung container terminals in Hong Kong. *Eur. J. Oper. Res.* **2002**, *140*, 1–11.
17. Canonaco, P.; Legato, P.; Mazza, R.; Musmanno, R. A queuing network model for the management of berth crane operations. *Comput. Oper. Res.* **2008**, *35*, 2432–2446.

18. Saeed, N.; Larsen, O. Application of queuing methodology to analyze congestion: A case study of the Manila International Container Terminal, Philippines. *Case Stud. Transp. Policy* **2016**, *4*, 143–149.
19. Noritake, M.; Kimura, S. Optimum allocation and size of seaports. *J. Waterw. Port Coast. Ocean Eng.* **1990**, *116*, 287–299.
20. Lee, W.; Cho, S. Reinforcement learning approach for outbound container stacking in container terminals. *Comput. Ind. Eng.* **2025**, *204*, 111069.
21. Lee, S.; Lee, S.H.; Choi, S.; Cho, S. Fuzzy C-means clustering based vertical container stacking in container terminals. *Sci. Rep.* **2026**, *16*, 6891.
22. Woo, S.; Park, H.; Cho, S.; Kim, K. Proactive berth scheduling with data-driven buffer time in container terminals. *Int. Trans. Oper. Res.* **2024**, *31*, 2875–2902.
23. Tsoulfas, G. Port resilience: A systematic literature review. *Marit. Econ. Logist.* **2026**, *28*, 388–408.
24. Li, L.; Wei, C.; Liu, J.; Chen, J.; Yuan, H. Assessing port cluster resilience: Integrating hypergraph-based modeling and agent-based simulation. *Transp. Res. Part D Transp. Environ.* **2024**, *136*, 104459.
25. Wei, Y.; Cheng, Y.; Liao, H.; Elsayed, E.A. Resilience modeling for an engineered network with multimodal performance under multiple recurrent hazards. *Reliab. Eng. Syst. Saf.* **2026**, *266*, 111640. https://doi.org/10.1016/j.ress.2025.111640.
26. Wei, Y.; Cheng, Y.; Liao, H. Optimal resilience-based restoration of a system subject to recurrent dependent hazards. *Reliab. Eng. Syst. Saf.* **2024**, *247*, 110137. https://doi.org/10.1016/j.ress.2024.110137.
27. Hapag-Lloyd. Europe Operational Updates—Week 7, 2026. Available online: https://www.hapag-lloyd.com/en/services-information/operational-updates/updates/2026/02/ops-updates-north-europe-week7.html (accessed on 2 November 2026).
28. Vukicevic Bisevac, I.; Vidic, N.; Vukadinovic, K. A Solution Approach to the Daily Dockworker Planning Problem at a Port Container Terminal. *Math. Probl. Eng.* **2021**, *2021*, 2359279. https://doi.org/10.1155/2021/2359279.
29. Amaran, S.; Sahinidis, N.; Sharda, B.; Bury, S. Simulation optimization: A review of algorithms and applications. *Ann. Oper. Res.* **2016**, *240*, 351–380.
30. Yeosu Regional Office of Oceans and Fisheries. General Overview: Port Facility Capacity (March 2026). Available online: https://yeosu.mof.go.kr/ko/page.do?menuIdx=3832 (accessed on 10 October 2026). (In Korean)
31. Ministry of Oceans and Fisheries. PORT-MIS Vessel Arrival and Departure Records: Fully Cellular Container Vessels at Busan and Gwangyang Ports, 2024. Available online: https://new.portmis.go.kr/ (accessed on April 7 2026). (In Korean)
32. World Bank.; S&P Global Market Intelligence. *The Container Port Performance Index 2023*; World Bank: Washington, DC, USA, 2024.
33. Yeosu Gwangyang Port Authority. 2024 Major Cargo Statistics of Yeosu and Gwangyang Ports. 2025. Available online: https://www.ygpa.or.kr/hmpg/ygpa/port/gymg/stat/bordContDetail.do?bbs_no=426&pst_no=92BBFEC63D114978B08A69999B0DE848 (accessed on 30 October 2026). (In Korean)
34. Busan Port Authority. Busan Port Authority Launches the Second Pilot Operation of the Transshipment Shuttle System (TSS). 5 July 2023. Available online: https://www.busanpa.com/board/view.do?boardId=BBS_0000031&dataSid=30268&menuCd=DOM_000000105002001000&paging=ok&startPage=104 (accessed on 29 September 2026). (In Korean)
35. Ministry of Data and Statistics. Consumer Price Index: Annual Inflation Rates and Monthly Index. Available online: https://mods.go.kr/menu.es?mid=b70202040000; https://mods.go.kr/cpidtval.es?mid=b70201010000 (accessed on 10 October 2026). (In Korean)
36. Brouer, B.; Alvarez, J.; Plum, C.; Pisinger, D.; Sigurd, M. A base integer programming model and benchmark suite for liner-shipping network design. *Transp. Sci.* **2014**, *48*, 281–312.
37. Zhao, Y.; Ye, J.; Zhou, J. Container fleet renewal considering multiple sulfur reduction technologies and uncertain markets amidst COVID-19. *J. Clean. Prod.* **2021**, *317*, 128361.
38. Ministry of Land, Infrastructure and Transport. Amended Notification on Safe Freight Rates for Application in 2026, 2026. Notification No. 2026-402; Republic of Korea, 2026. Available online: https://www.molit.go.kr/USR/I0204/m_45/dtl.jsp?idx=18923 (accessed on 29 September 2026). (In Korean)
39. Adi, T.; Bae, H.; Iskandar, Y. Interterminal truck routing optimization using cooperative multiagent deep reinforcement learning. *Processes* **2021**, *9*, 1728.
40. Hou, W.; Shi, Q.; Guo, L. Impacts of COVID-19 pandemic on foreign trade intermodal transport accessibility: Evidence from the Yangtze River Delta region of mainland China. *Transp. Res. Part A Policy Pract.* **2022**, *165*, 419–438. https://doi.org/10.1016/j.tra.2022.09.019.

Disclaimer/Publisher's Note: The statements, opinions and data contained in all publications are solely those of the individual author(s) and contributor(s) and not of MDPI and/or the editor(s). MDPI and/or the editor(s) disclaim responsibility for any injury to people or property resulting from any ideas, methods, instructions or products referred to in the content.